# Nonlinear instabilities in a vertical pipe flow discharging from a cylindrical container

E. Sanmiguel-Rojas
*Universidad Politécnica de Cartagena, E.T.S. Ingenieros Industriales, 30202 Cartagena, Murcia, Spain*

R. Fernandez-Feria
*Universidad de Málaga, E.T.S. Ingenieros Industriales, 29013 Málaga, Spain*

(Received 18 May 2005; accepted 3 January 2006; published online 1 February 2006)

We report results from three-dimensional numerical simulations of the incompressible flow in a vertical pipe of circular cross-section discharging from a cylindrical container. Natural Coriolis forces due to Earth rotation trigger the instability of the axisymmetric flow, and nonlinear spiral waves with azimuthal wave number $|n|=3$ are formed above a critical Reynolds number based on the pipe flow rate ($\mathrm{Re}_Q$). We characterize this critical Reynolds number as a function of the Coriolis parameter ($F$), that is proportional to the square of the radius of the container. As a difference with previous numerical works on nonlinear instabilities and transition in a pipe flow, here the nonlinear disturbances needed to trigger the instabilities are not artificially introduced inside the pipe flow, but naturally produced by Coriolis forces, the amplitude of these disturbances being characterized by a nondimensional Coriolis parameter. We find that the pipe flow can be unstable for $\mathrm{Re}_Q$ as low as 300 for the largest value of $F$ considered. We also discuss the relevance of the residual swirl introduced by natural Coriolis forces in triggering the nonlinear traveling waves. © *2006 American Institute of Physics*. [DOI: 10.1063/1.2168445]

## I. INTRODUCTION

Recent theoretical, numerical, and experimental works have reported the existence of nonlinear traveling waves in pipe flow at relatively low Reynolds numbers, and their significance to the transition to turbulent pipe flow.[1–3] To generate the instabilities that produces such nonlinear waves and, at the end, a turbulent flow, both in experiments and in numerical simulations, several disturbance generators and their numerical counterparts have been envisaged downstream the pipe inlet.[4–7] In this work we add further knowledge to the formation on nonlinear traveling waves in a pipe flow by direct numerical simulation of the flow in a vertical pipe discharging from a container without the use of any artifact to generate and introduce the nonlinear disturbances into the flow. The instabilities are triggered by natural Coriolis forces, whose intensity at the pipe inlet is controlled by varying the size of the container. In addition, as a difference with other numerical simulations,[4,7] no damping zone near the pipe outlet is required to impose the outflow boundary condition because no velocity boundary conditions are needed in the numerical method used here: the flow evolves freely from a given pressure difference between the inlet surface at the container and the pipe outlet, without any other constraint at the outflow boundary.[8] This numerical technique has been successfully used recently to describe nonlinear traveling waves in a rotating pipe.[9] Here the tank-pipe system does not rotate, though a swirl velocity component is introduced locally at the pipe inlet by natural Coriolis forces, whose intensity is proportional to the square of the radius of the tank. We discuss in the last section the significance of this residual swirl in triggering the nonlinear instabilities.

## II. FORMULATION OF THE PROBLEM

We solve numerically the three-dimensional, incompressible Navier-Stokes equations, including natural Coriolis body forces due to Earth rotation, which in dimensionless form can be written as

$$\nabla \cdot \mathbf{v} = 0, \tag{1}$$

$$\frac{\partial \mathbf{v}}{\partial t} + \mathbf{v} \cdot \nabla \mathbf{v} = -\nabla p + \frac{1}{\mathrm{Re}}(\nabla^2 \mathbf{v} - F\mathbf{e}_z \wedge \mathbf{v}), \tag{2}$$

in the domain depicted in Fig. 1, which consists on a pipe of length $l$ and diameter $d$ discharging from a coaxial cylindrical container of radius $R$. The axes of both the pipe and the container are parallel to the vertical axis $\mathbf{e}_z$, and we have selected a pipe length $l=20d$. Cylindrical-polar coordinates $(r,\theta,z)$, with velocity field $\mathbf{v}=(u,v,w)$, are used. The flow is

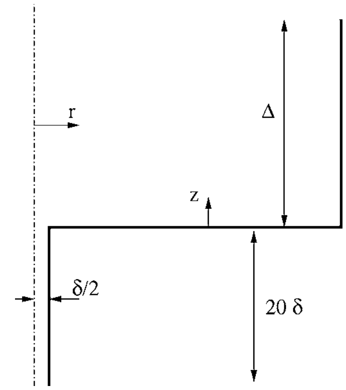


FIG. 1. Nondimensional integration domain and coordinates.

 

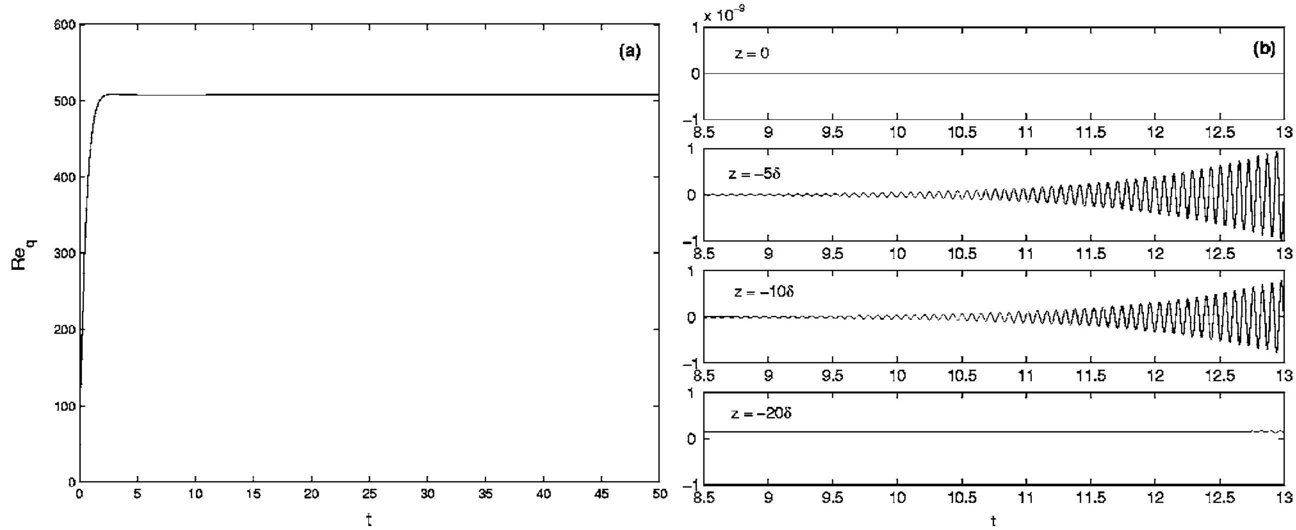

FIG. 2. (a) $\mathrm{Re}_q(t)$ for $\mathrm{Re}_Q=508$ (Re=20 000) and $F=1000$. (b) $v(r=\delta/4,\theta=0,z)-v(r=\delta/4,\theta=\pi,z)$ as function of $t$ for different values of $z$ inside the pipe, as indicated ($\mathrm{Re}_Q=508$, $F=1000$).

produced by a pressure difference $\Delta p_c$, which includes gravity forces ($p$ is the nondimensional reduced pressure), between some height $H$ above the base of the container and the pipe exit. Accordingly, we define a characteristic velocity based on this pressure difference, $V_c \equiv \sqrt{\Delta p_c/\rho}$, where $\rho$ is the fluid density, which, together with the length scale $R$, are used to nondimensionalize the equations and boundary conditions. Thus, the Reynolds number Re and the Coriolis parameter $F$ in Eq. (2) are defined as

$$\mathrm{Re} = \frac{\sqrt{\Delta p_c/\rho}R}{\nu}, \quad F = \frac{fR^2}{\nu}, \tag{3}$$

where $\nu$ is the kinematic viscosity of the fluid and $f \equiv 2\Omega \sin\phi$ is the Coriolis frequency at the given latitude $\phi$. The nondimensional boundary conditions are the following (see Fig. 1): zero velocity at the solid walls,

$$\mathbf{v} = 0 \text{ at } \begin{cases} r = 1, \quad 0 \leqslant z \leqslant \Delta, \qquad \Delta \equiv \dfrac{H}{R}, \\ \delta/2 \leqslant r \leqslant 1, \quad z = 0, \qquad \delta \equiv \dfrac{d}{R}, \\ r = \delta/2, \quad -20\delta \leqslant z \leqslant 0; \end{cases} \tag{4}$$

and given pressure at the center of the inlet and outlet sections,

$$\begin{aligned} p &= 1 \quad \text{at } r = 0, \quad z = \Delta, \\ p &= 0 \quad \text{at } r = 0, \quad z = -20\delta. \end{aligned} \tag{5}$$

We start with the fluid at rest ($\mathbf{v}=0$ at $t=0$). The pressure difference between the inlet section at $z=\Delta$ and the pipe outlet, $z=-20\delta$, sets the fluid into motion without any other constraint on these sections, so that the fluid velocity evolves freely at the pipe outlet. For details on the numerical technique, see Refs. 8 and 9. In the computations we have selected $\delta=0.04$, $\Delta=1.5$, and a nonuniform grid with $n_r=114 \times n_\theta=10 \times n_z=351$ nodes concentrated near the pipe inlet ($z=0$, $0 \leqslant r \leqslant \delta/2$). Second-order finite-differences both in space and time (time step $\Delta t=2\times 10^{-4}$) are used on the nonuniform mesh.[10]

Though in the computations we use the Reynolds number (3) based on the pressure difference, the results given below are presented in terms of the usual Reynolds number based on the flow rate $Q$, and the pipe diameter $d$, $\mathrm{Re}_Q = 4Q/(\pi d\nu)$. To obtain it, we compute the flow rate at the pipe exit at each instant of time. In nondimensional form,

$$\mathrm{Re}_q(t) = \mathrm{Re}\,\frac{4}{\pi\delta}\int_0^{2\pi}\int_0^{\delta/2}[rw]_{z=-20\delta}\,dr\,d\theta. \tag{6}$$

This quantity tends to $\mathrm{Re}_Q$ if a steady state is reached. Otherwise, we use the maximum value reached by $\mathrm{Re}_q$ before nonlinear traveling waves are developed in the pipe flow.

## III. RESULTS

For a given value of the Coriolis parameter $F$ (a given value of the radius of the cylindrical container $R$, say), we increase $\mathrm{Re}_Q$ (i.e., we increase the pressure difference through Re). For low Reynolds numbers, the flow evolves in time until an *axisymmetric* steady state is reached. However, above a critical Reynolds number, which depends on $F$, $\mathrm{Re}_Q^c(F)$, the flow becomes unstable somewhere inside the pipe at some instant of time, and nonaxisymmetric traveling waves are formed. This situation is illustrated here for $F=1000$ (for water in middle latitudes, this value of $F$ corresponds to a container of about $4m$ of radius). We find that the flow remains axisymmetric throughout the domain up to $\mathrm{Re}_Q^c(1000) \simeq 490$. Above this Reynolds number, the flow becomes unstable inside the pipe just after the nominal flow rate is reached. For instance, for Re=20 000, the nominal flow rate, corresponding to $\mathrm{Re}_Q=508$, is reached at about $t=2.5$ [Fig. 2(a)]. Just after that, at $t$ between 8 and 8.5, the flow becomes unstable to nonaxisymmetric perturbations inside the pipe, first at $z\sim -5\delta$, as it can be seen in Fig. 2(b),

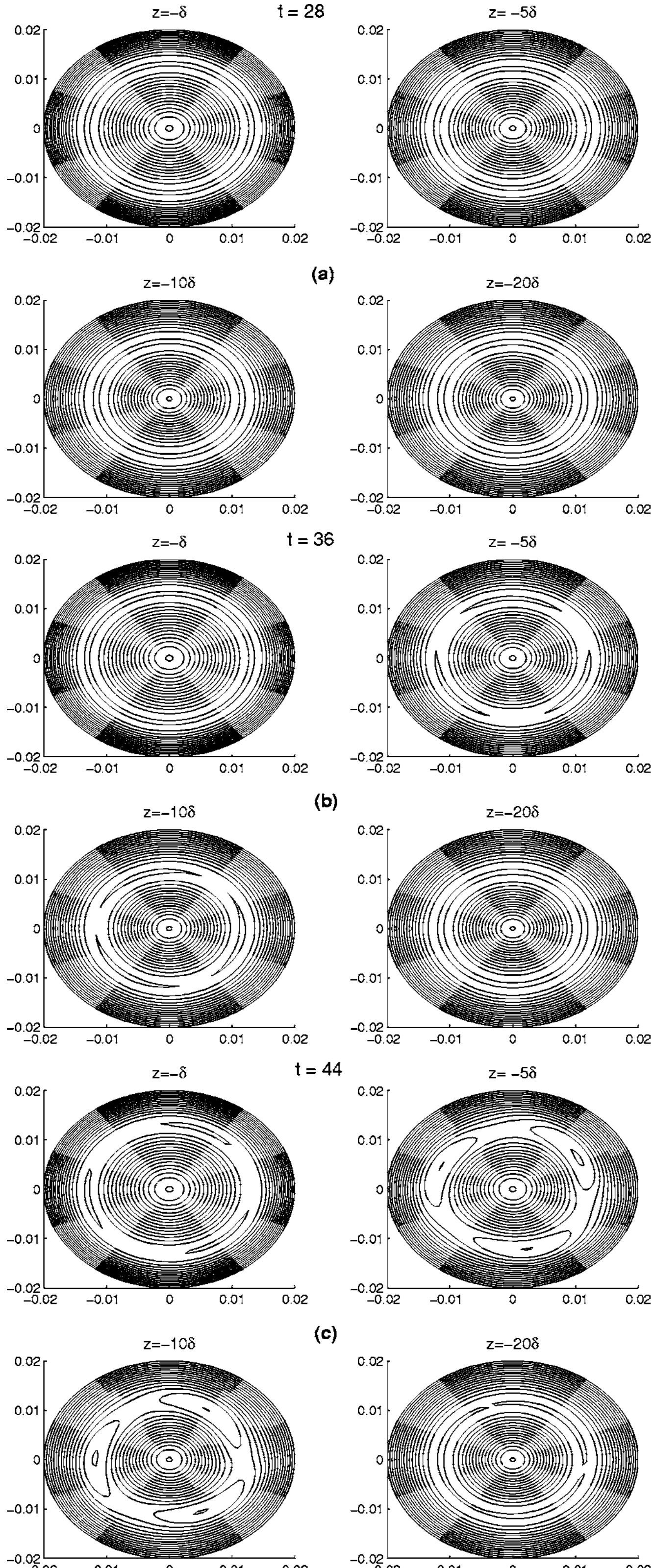


FIG. 3. Contour lines of the circulation $vr$ in four $r\theta$ sections of the pipe ($z=-\delta$, $z=-5\delta$, $z=-10\delta$, and $z=-20\delta$) for $\mathrm{Re}_Q=508$, $F=1000$, and three instants of time $t$ at (a) 28, (b) 36, and (c) 44.

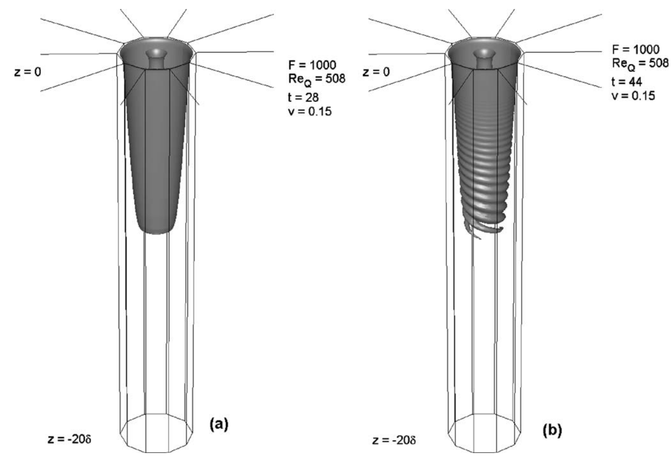


FIG. 4. Three-dimensional view of the isosurfaces $v=0.15$ in the pipe for $\mathrm{Re}_Q=508$ and $F=1000$ at two instants of time $t$ at (a) 28 and (b) 44.

where we plot the difference between the azimuthal velocities at $\theta=0$ and at $\theta=\pi$ for several values of $z$ as a function of time. It is observed that the perturbations grow exponentially in time at each axial location and travel downstream. For $t=28$, the amplitude of these perturbations are still too small for being appreciated in a contour map of the azimuthal velocity [see Fig. 3(a), where we plot the contour lines of the circulation $vr$; note that the amplitude of the nonaxisymmetric waves in Fig. 2(b) is very small, of the order of $10^{-9}$]. However, at $t=36$, the amplitude of the nonlinear waves has grown enough to be already appreciable at the central sections of the pipe [see Fig. 3(b)]. Later, at $t=44$, they can be observed all along the pipe [Fig. 3(c)]. This is better appreciated in Fig. 4, where the isosurfaces corresponding to $v=0.15$ are plotted inside the pipe.

It is observed that the nonlinear wave formed after the instability of the flow inside the pipe corresponds to a spiral wave with azimuthal wave number $|n|=3$. The waves are counter-rotating ($n=-3$) in relation to the inlet ($z=0$) mean flow, which has a positive azimuthal velocity [see Fig. 5(c)], in accordance with the Coriolis forces in the northern hemisphere. Also plotted in Fig. 5 are, for reference sake, the

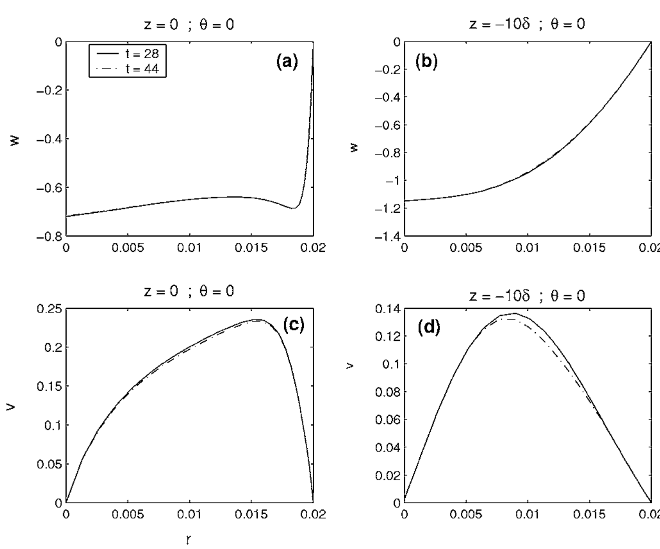


FIG. 5. Axial ($w$) and azimuthal ($v$) radial velocity profiles for $\theta=0$ at the pipe inlet ($z=0$) and at the middle of the pipe ($z=-10\delta$) for two instants of time, as indicated. $\mathrm{Re}_Q=508$, $F=1000$.

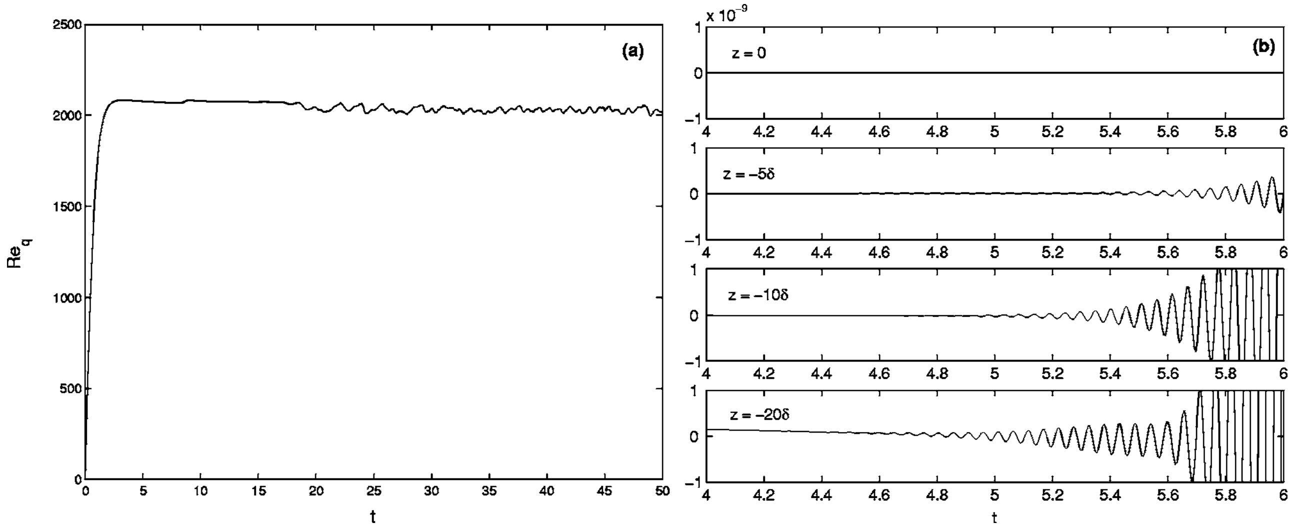


FIG. 6. As in Fig. 2, but for $\mathrm{Re}_Q$=2050 (Re=60 000).

radial profile of the axial velocity at the pipe inlet, and both the axial and the azimuthal radial velocity profiles at the mid section of the pipe. It is observed that the profile of the axial velocity is almost flat at the pipe inlet [Fig. 5(a)], becoming parabolic inside [Fig. 5(b)]. The magnitude of the azimuthal velocity at the pipe inlet is about four times smaller than the axial velocity for the values $F=1000$ and $\mathrm{Re}_Q=508$ considered. The differences in the azimuthal velocities for the two instants of time plotted are due to the nonlinear traveling waves formed inside the pipe.

For higher Reynolds numbers, the evolution of the flow is qualitatively similar. The main differences are, as shown in Figs. 6–9 for $\mathrm{Re}_Q=2050$ (Re=60 000), that the instability develops earlier in time, and that the nonlinear traveling waves are quite more intense. But these traveling waves are still spiral waves with azimuthal wave number $|n|=3$ (no other value of the azimuthal wave number have been observed in the present numerical simulations). Another difference is that the flow rate (i.e., $\mathrm{Re}_Q$) decreases more, and undergoes more accused oscillations, than in the previous case after the formation of the nonlinear waves [compare Fig. 2(a) with 6(a)]. This is obviously due to the enhanced friction produced by the traveling waves, that reduces the flow rate for the given (fixed) pressure difference.

We have repeated the computations for several values of $F$ and have characterized the critical Reynolds number at which the pipe flow becomes unstable as a function of $F$. The results are summarized in Fig. 10. We have been able to pursue the computations up to $\mathrm{Re}_Q \simeq 3200$, and up to $F=4000$. The logarithmic plot in Fig. 10(b) shows that the critical amplitude of the perturbations ($F$) for instability do not follow an unique power law of the type $\mathrm{Re}^{-\lambda}$ in the range of Re considered. It is observed that the flow becomes unstable for relatively small values of $\mathrm{Re}_Q$ if $F$ is large enough ($\mathrm{Re}_Q^c \simeq 300$ for $F=4000$), and that for $F \to 0$ the critical value of $\mathrm{Re}_Q$ tends to infinity.

## IV. CONCLUSION

We have shown that Coriolis forces may trigger instabilities and the formation of nonlinear traveling waves in a pipe flow discharging from a cylindrical container at relatively low Reynolds numbers. The critical Reynolds numbers for the onset of these waves have been characterized as a function of the Coriolis parameter $F$ in a wide range of $F$.

These results may be compared with the recent stability results by Herrada *et al.*[11] for a swirling flow decaying in a circular pipe. These authors consider the spatial stability, at the entrance region of a pipe, of the flow developing from an uniform axial velocity together with a Burgers-like vortex of variable swirl strength and core radius at the pipe inlet. These inlet flows have certain similarities with those depicted in Figs. 5(a), 5(c), 9(a), and 9(c) at the pipe inlet in the present numerical simulations. However, the stability results in Ref. 11 show that the most unstable perturbations are counter-rotating ones with azimuthal wave number $n=-1$, becoming unstable at a critical Reynolds number of a few hundreds, depending on the swirl strength and the core radius of the inlet Burgers vortex. In our numerical simulations we have searched for nonaxisymmetric instabilities in every section of the pipe and at every instant of time, and we have only detected instabilities with azimuthal wave number $|n|=3$. This qualitative discrepancy may be due (in addition to the obvious quantitative differences between the inlet flows) to the fact that the centrifugal linear instabilities reported in Ref. 11 are quite localized near the pipe inlet, whereas the nonlinear instabilities found here develop several pipe diameters downstream.

Helical waves in a circular pipe have also been numerically searched by Landman,[12] who looked for helically symmetric solutions to the Navier-Stokes equations, finding also that a residual swirl may generate these waves. But, in consonance with linear stability analyses of pipe flow with a superposed swirling core,[11,12] (or even with a rotating pipe flow, see, e.g., Mackrodt),[13] the waves found by this author

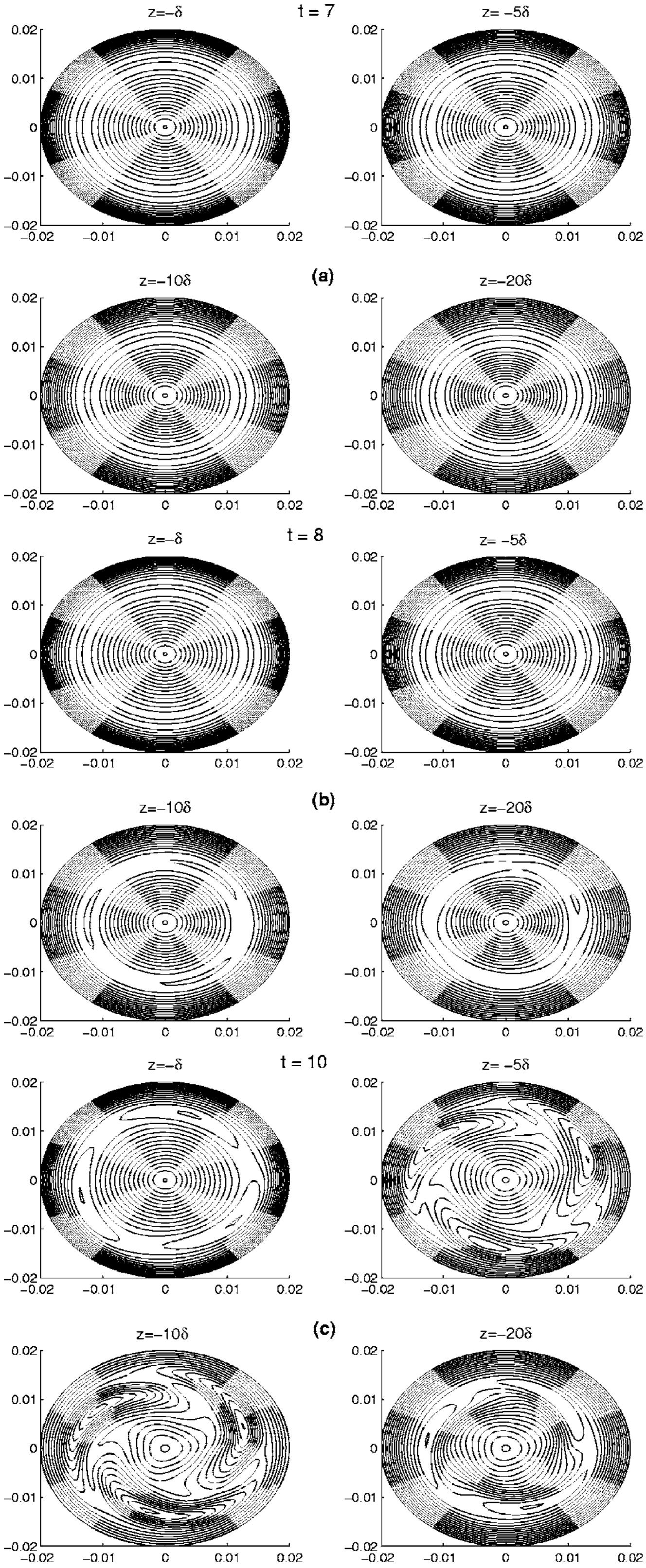


FIG. 7. As in Fig. 3, but for $\mathrm{Re}_Q=2050$, and for $t$ at (a) 7, (b) 8, and (c) 10.

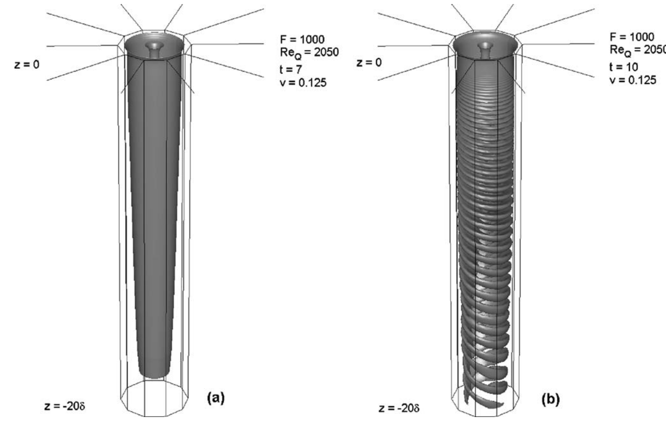


FIG. 8. As in Fig. 4, but for $\mathrm{Re}_Q=2050$, for $v=0.125$, and for $t$ at (a) 7 and (b) 10.

have azimuthal wave number $|n|=1$ (or $|n|=2$ in some cases). Thus, we tentatively conclude that the nonlinear traveling waves reported here from a full *numerical experiment* in a pipe flow discharging from a tank are more connected to those recently described for pipe Poiseuille flow at relatively low Reynolds numbers[1–3] than to *linear* instabilities of a pipe flow with superposed swirl. The instabilities are triggered here by the nonlinear disturbances introduced into the pipe flow by natural Coriolis forces, which are particularly intense near the pipe inlet as $F$ increases. The $(n=3)$ waves persist along the pipe (exiting from it) if the Reynolds number is high enough. Though we have checked this result using a longer pipe than that reported here, with $l=30d$ and even $40d$, more definitive results would require a much longer pipe, which is presently unreachable with our present computer facilities. What is definitely independent of the pipe length is the neutral curve depicted in Fig. 10 for a wide range of $F$, and the azimuthal wave number $|n|=3$ of the nonlinear waves.

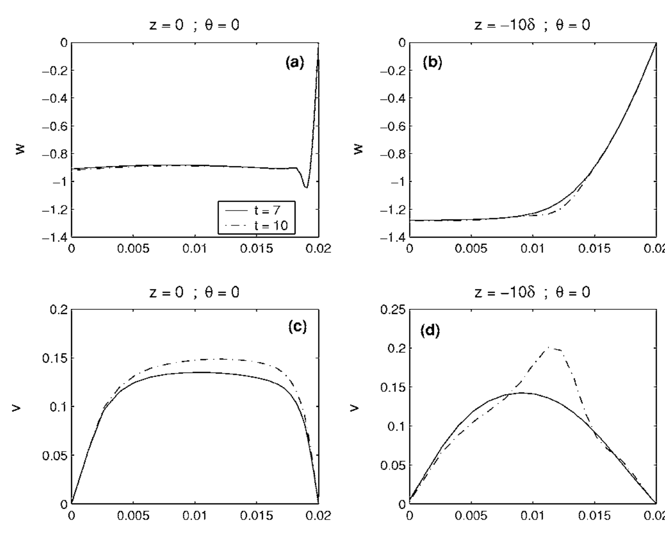


FIG. 9. As in Fig. 5, but for $\mathrm{Re}_Q=2050$.

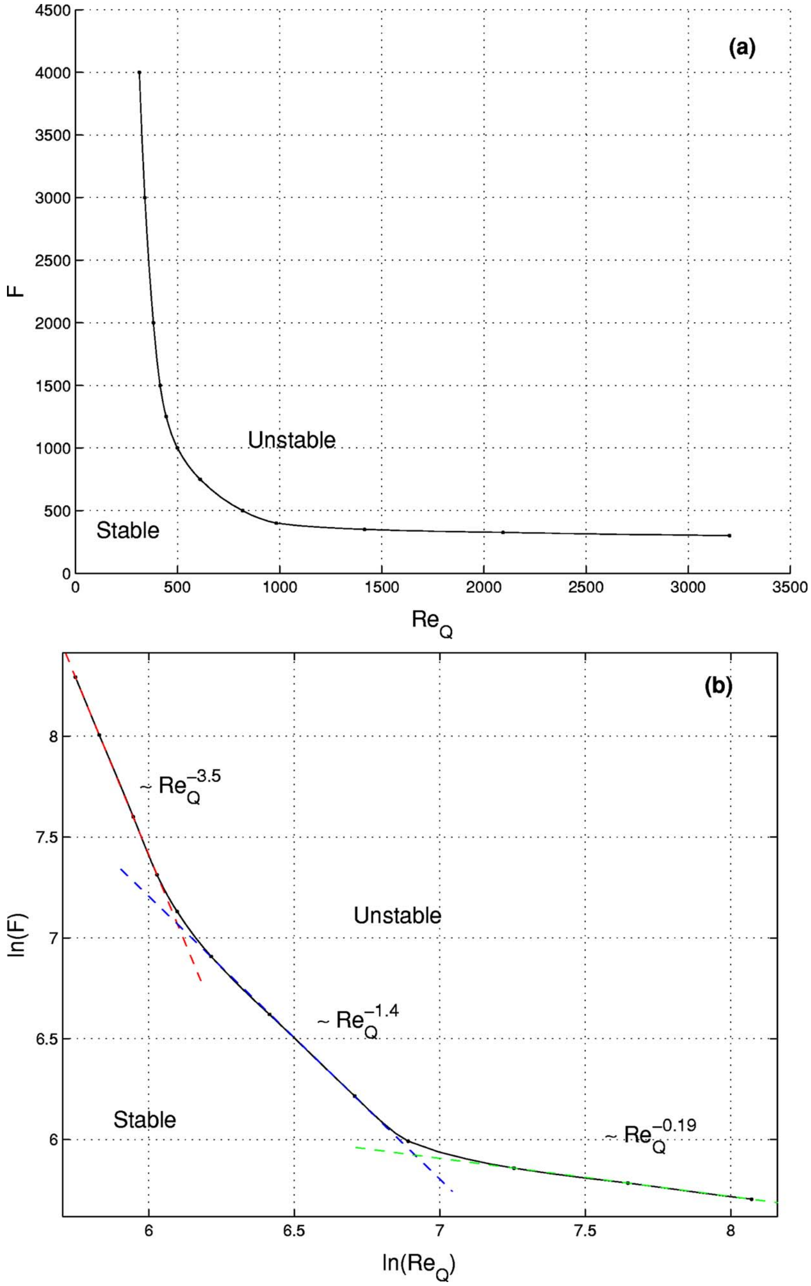


FIG. 10. Instability region in the plane $\mathrm{Re}_Q - F$. (a) Linear plot and (b) logarithmic plot showing the different scaling laws.

## ACKNOWLEDGMENTS

This work have been supported by the Ministerio de Educación y Ciencia of Spain (Grant No. FIS2004-00538). All the numerical computations have been made in the computer facilities at the SAIT (U.P. Cartagena).

[1]H. Faisst and B. Eckhardt,"Traveling waves in pipe flow, "Phys. Rev. Lett. **91**, 224502 (2003).

[2]H. Wedin and R. R. Kerswell, "Exact coherent structures in pipe flow: travelling wave solutions," J. Fluid Mech. **508**, 333 (2004).

[3]B. Hof, C. W. H. van Dorne, J. Westerweel, F. T. M. Nieuwstadt, H. Faisst, B. Eckhardt, H. Wedin, R. R. Kerswell, and F. Waleffe, "Experimental observation of nonlinear traveling waves in turbulent pipe flow,"Science **305**, 1594 (2004).

[4]B. Ma, C. W. H. van Doorne, Z. Zhang, and F. T. M. Nieuwstadt, "On the spatial evolution of a wall-imposed periodic disturbance in pipe Poiseuille flow at Re=3000. Part 1. subcritical disturbance," J. Fluid Mech. **398**, 181 (1999).

[5]G. Han, A. Tumin, and I. Wygnanski, "Laminar-turbulent transition in Poiseuille pipe flow subjected to periodic perturbation emanating from the wall. Part 2. Late stage of transition," J. Fluid Mech. **419**, 1 (2000).

[6]B. Hof, A. Juel, and T. Mullin, "Scaling of the turbulence transition threshold in a pipe," Phys. Rev. Lett. **91**, 244502 (2003).

[7]J. Reuter and D. Rempfer, "Analysis of pipe flow transition. Part I. Direct numerical simulation," Theor. Comput. Fluid Dyn. **17**, 273 (2004).

[8]R. Fernandez-Feria and E. Sanmiguel-Rojas, "An explicit projection method for solving incompressible flows driven by a pressure difference," Comput. Fluids **33**, 463 (2004).

[9]E. Sanmiguel-Rojas and R. Fernandez-Feria, "Nonlinear waves in the pressure driven flow in a finite rotating pipe," Phys. Fluids **17**, 014104 (2005).

[10]E. Sanmiguel-Rojas, J. Ortega-Casanova, C. del Pino, and R. Fernandez-Feria, "A cartesian grid finite-difference method for 2d incompressible viscous flows in irregular geometries," J. Comput. Phys. **204**, 302 (2005).

[11]M. A. Herrada, M. Perez-Saborid, and A. Barrero, "Nonparallel local spatial stability analysis of pipe entrance swirling flows," Phys. Fluids **16**, 2147 (2004).

[12]M. J. Landman, "On the generation of helical waves in circular pipe flow," Phys. Fluids A **2**, 738 (1990).

[13]P. A. Mackrodt, "Stability of Hagen-Poiseuille flow with superimposed rigid rotation," J. Fluid Mech. **73**, 153 (1976).